TR-WEL-0006

004

Evaluation of Continuous-Phase Frequency-Shift Keying Schemes for a Gigabit WLAN

Thomas Hunziker

2005.2.17

(株)国際電気通信基礎技術研究所
波動工学研究所
〒619-0288 京都府相楽郡精華町光台二丁目 2 番地 2
Tel: 0774-95-1501 Fax: 0774-95-1508

Advanced Telecommunications Research Institute International
Wave Engineering Laboratories
2-2-2 Hikaridai, Seika-cho, Soraku-gun, Kyoto 619-0288, Japan
Telephone: +81-774-95-1501 Fax: +81-774-95-1508

Abstract

This report contains a study on continuous-phase frequency-shift keying (CPFSK) based transmission for Gigabit WLANs in millimeter-wave bands. The error rate performance of CPFSK signals in combination with noncoherent receivers and their bandwidth consumption are investigated. Based on the obtained results, adequate transmission schemes for achieving up to 4 Gbit/s while using at most 3 GHz of bandwidth are identified.

Contents

1. Introduction

Wireless LANs operating around 60 GHz may in the future achieve data rates far beyond the maximum 54 Mbit/s of the IEEE 802.11a standard for instance. A system offering up to 4 Gbit/s is envisaged in [1]. This ambitious goal makes high demands on the analog and digital devices. Efficient power amplifiers are necessary among other things in view of the small antenna apertures at 60 GHz, suggesting the adoption of a modulation scheme with constant envelope. And the demodulation and decoding of the high-speed data are a challenge for the digital baseband processing unit in the receivers. Only noncoherent receivers may be considered at first due to their limited complexity.
Continuous-phase frequency-shift keying (CPFSK) is an advantageous modulation method as the resulting signals have constant envelope and a noncoherent reception is possible. In the following, the error rate and bandwidth performance of CPFSK schemes are investigated, assuming noncoherent receivers, and auspicious modulation schemes are identified.

2. Continuous-Phase Frequency-Shift Keying (CPFSK)

Frequency-shift keying (FSK) is a *memoryless* modulation method. In the case of M-ary FSK, the kth symbol $I_k \in \{-(M-1),-(M-3),...,(M-1)\}$ maps to the waveform

$$s_k(t;I_k) = A\exp\left(j\pi I_k h(t-kT)/T\right), \quad t \in [kT,(k+1)T),$$

where h represents the modulation index, T defines the symbol duration, and A is a constant. The envelope of a FSK baseband signal is constant, however, the phase may be non-continuous. As this induces large side lobes, a continuous-phase (CP) version of FSK, termed CPFSK, is more widely used. The phase at the beginning of every symbol interval depends on the previous symbols, hence, CPFSK is a modulation method *with memory*. A CPFSK signal can be generated using an integrator and a phase modulator. To even further improve the spectral properties, a low-pass filter may be employed prior to the modulator. Figure 1 shows a block diagram of a CPFSK transmitter including the up-conversion to the radio frequency (RF).

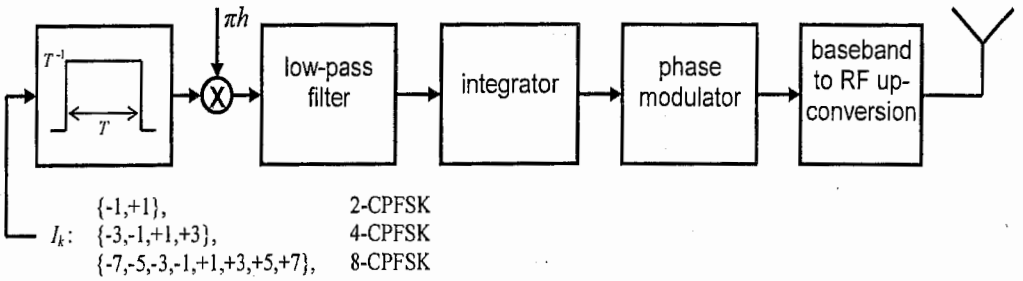

Figure 1: CPFSK transmitter model.

Many types of low-pass filters attenuate the side lobes. One possible choice are Gaussian filters with impulse responses of the form

$$f_G(t) = C\exp\left(-\frac{\pi^2}{2\log(2)}(B_{3dB}T)^2\left(\frac{t}{T}\right)^2\right),$$

where B_{3dB} defines the half-power bandwidth, and C is a constant. Employing CPFSK with a modulation index of $h = 0.5$ is usually termed *minimum-shift keying* (MSK), and combining MSK with a Gaussian filter is referred to as *Gaussian MSK*, which was for example adopted by GSM.

3. CPFSK Receivers

Both coherent and noncoherent CPFSK receivers are available. Coherent receivers achieve superior performance, but their complexity may be prohibitive. Noncoherent receivers do not need signal phase recovery prior to the detection, and they are attractive when the carrier recovery circuit is difficult to implement, as is the case for high frequency signals such as millimeter-waves. A further approach is differential detection, which is a mixture of coherent and non-coherent techniques.

Figure 2 shows a model of a generic noncoherent detector. After the translation into the baseband, the received signal is cross-correlated against the elementary noise-free pulse shapes. Rather than utilizing the complex-valued coefficients from the correlators, their outputs are envelope-detected, thus lacking phase information.

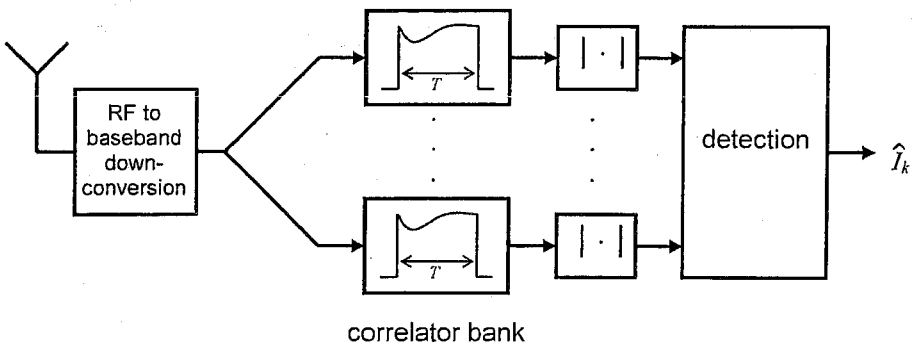

Figure 2: Generic noncoherent receiver.

A low-pass filtering before the CPFSK modulation causes inter-symbol interference (ISI), and the support of the functions underlying the correlators exceeds a symbol interval. As a consequence, the correlator outputs for every symbol contain contributions from D subsequent symbols, where D depends on the length of the low-pass filter impulse response. The noncoherent CPFSK detector discussed in [2] employs M^{1+D} correlators to account for this overlapping. For each of the M possible symbols of the kth interval there are M^D correlators, one for every possible combination of subsequent symbols, and the maximum of the M^D correlator outputs is used for the detection.

The receiver complexity can be scaled down at the cost of some performance degradation by employing only M correlators, analyzing the signal over one symbol interval while neglecting ISI. Such a theoretical receiver also more closely resembles practical implementations of noncoherent detectors utilizing limiter and discriminator devices.
Multi-path signal propagation leads to echoes, which may have a significant effect on the receiver performance. Using a coherent receiver with maximum-likelihood sequence estimation, the presence of echoes may even improve the error rate performance. For noncoherent receivers, on the other hand, multi-path signal propagation is usually destructive.

4. Error Rate Performance of Noncoherent Receivers

In this study only transmission scenarios without multi-path signal propagation are considered, having an ideal channel between transmitter and receiver. The low-pass filtered signal belonging to the kth symbol is given as $(f_G * s_k)(t;I_k)$. The M-ary CPFSK detector considered in the following correlates the observed signal against the M waveforms $\{(f_G * s_k)(t;I_k), I_k \in \{-(M-1),...,(M-1)\}\}$ within the time interval $t \in [kT+t_0,(k+1)T+t_0)$, and detects the kth symbol by choosing the maximum of the M correlator output magnitudes. The constant t_0 defines the position of the correlation window of length T, and t_0 is chosen such that the ratio of the desired signal energy over the mean-squared error due to the ISI is maximal. For CPFSK signals with minor ISI, the performance of this detector is expected representative for a limiter-discriminator based receiver. A more detailed study on the performance of limiter-discriminator and differential detection schemes is found in [3].
The achievable error rate performance depends on the following system parameters:

- relative Gauss filter bandwidth $B_{3dB}T$
- modulation index h
- modulation level M
- signal-to-noise ratio (SNR) ε_S/N_0 at the receiver.

Figure 3 shows the numerically obtained symbol error rates (SERs) for 2-ary and 4-ary CPFSK versus the modulation index, assuming $B_{3dB}T = 1/2$ and a SNR equal 20dB. And Figure 4, Figure 5, Figure 6 show the corresponding results for Gauss filter bandwidths of $B_{3dB}T = 1, 2, 3$, including 8-ary CPFSK.
Obviously, with a $B_{3dB}T$ product of 0.5, only binary signaling in combination with a modulation index near 1 achieves acceptable error rates in the order of 10^{-3}. This is because of the relatively low temporal concentration of the Gauss filter response, leading to severe ISI. If $B_{3dB}T$ equals 1, the Gauss filter response is more concentrated in time, resulting in better error performance at the cost of a broader power spectrum in the frequency domain. And with a $B_{3dB}T$ product of 2 or 3, even 8-ary CPFSK signals can be detected at error rates below 10^{-3}, provided h is sufficiently large.

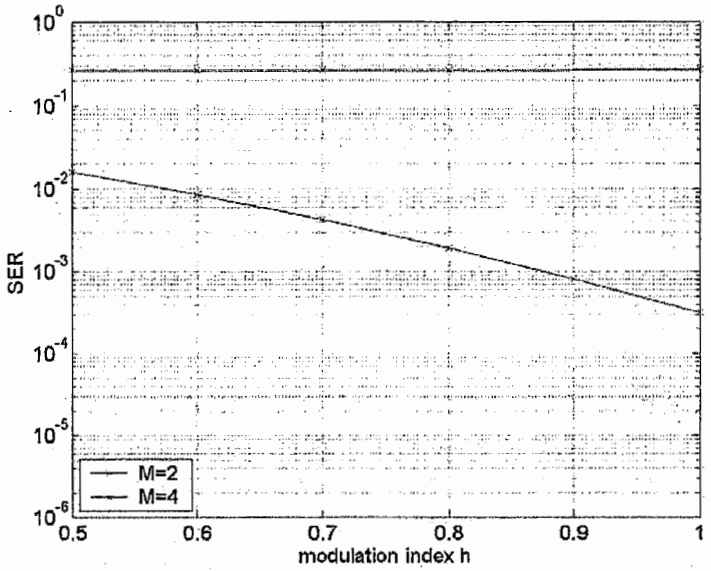

Figure 3: Symbol error rates versus h for $B_{3dB}T = 0.5$ and ε_S/N_0 equal 20dB.

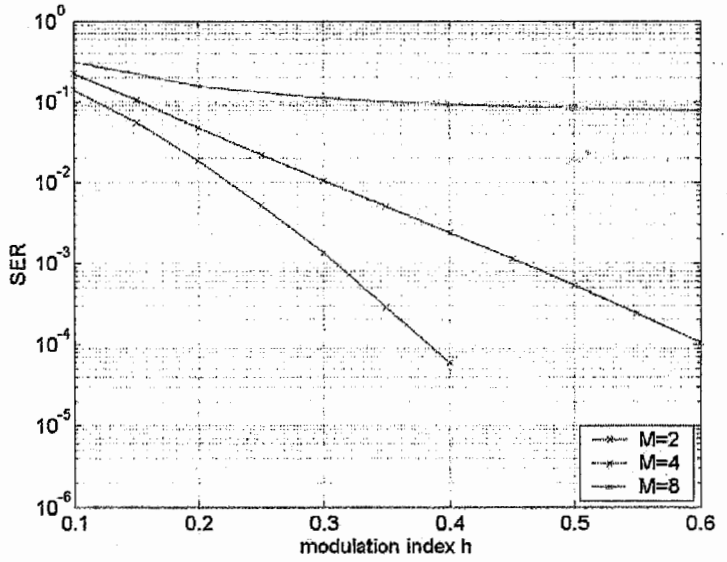

Figure 4: Symbol error rates versus h for $B_{3dB}T = 1.0$ and ε_S/N_0 equal 20dB.

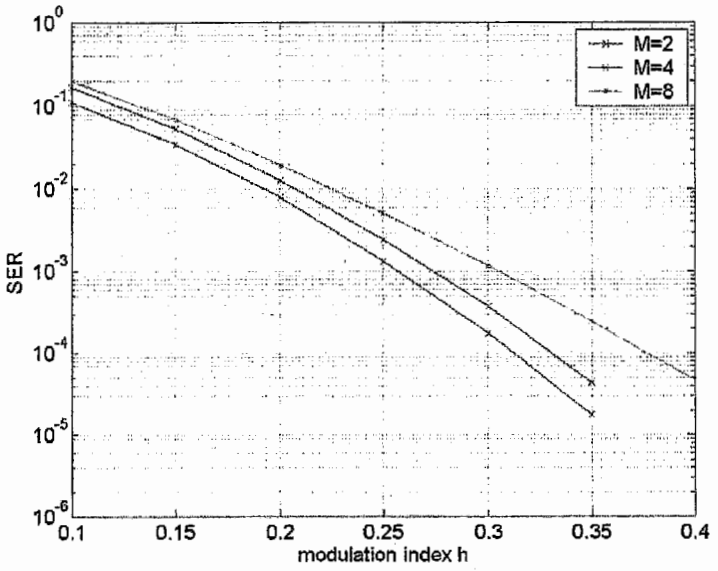

Figure 5: Symbol error rates versus h for $B_{3dB}T = 2.0$ and ε_S/N_0 equal 20dB.

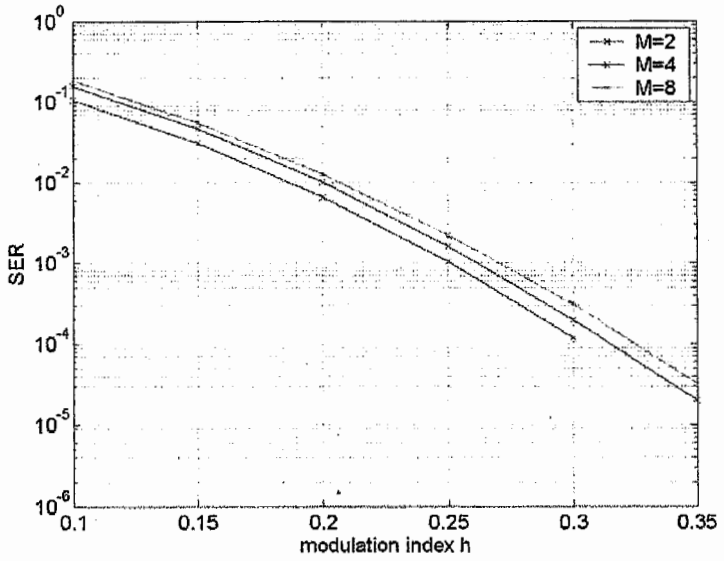

Figure 6: Symbol error rates versus h for $B_{3dB}T = 3.0$ and ε_S/N_0 equal 20dB.

Figure 7 shows the SERs for $B_{3dB}T = 3$ and a SNR of 12 dB. Here, the thermal noise is the limiting factor rather than the ISI. This can be seen in Figure 8, representing the case of $B_{3dB}T = 100$, which is equivalent to the absence of a low-pass filtering. Minimal error rates are attained at $h = 1$ as this results in orthogonal waveforms.

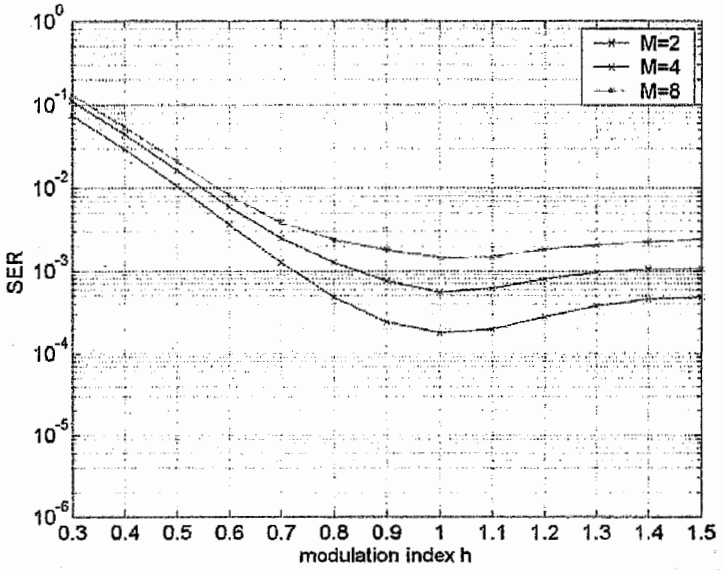

Figure 7: Symbol error rates versus h for $B_{3dB}T = 3.0$ and ε_S/N_0 equal 12dB.

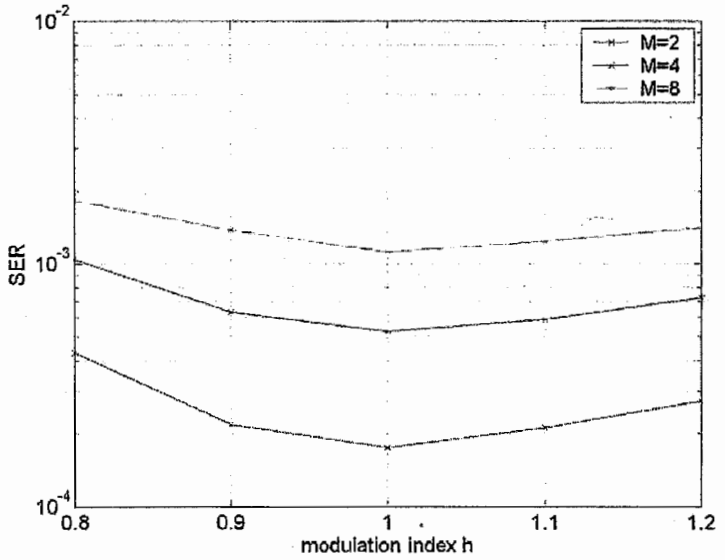

Figure 8: Symbol error rates versus h for $B_{3dB}T = 100$ and ε_S/N_0 equal 12dB.

5. Bandwidth of CPFSK Signals

The power spectrum of CPFKS signals can be computed as in [2], eqn. (4-4-30)-(4-4-33). An infinite CPFSK signal can be expressed as $s(t) = A\exp(j\varphi(t))$ with the phase

$$\varphi(t) = \sum_{k=-\infty}^{\infty} I_k \pi h q(t-kT),$$

where

$$q(t) = \int_{-\infty}^{t} p(\tau)d\tau$$

and $p(t)$ represents the pulse shape normalized to $\int_{-\infty}^{\infty} p(\tau)d\tau = 1$. The pulse shape $p(t)$ results from convolution of a function with a length T rectangular shape and the low-pass filter response $f_G(t)$. The autocorrelation $R(t+\tau,t) = E\left[s(t+\tau)s(t)^*\right]$ is found as

$$R(t+\tau,t) = |A|^2 \prod_{k=-\infty}^{\infty} \frac{1}{M} \sum_{m=-(M-1),-(M-3),\ldots,(M-1)} \exp\left(j\pi h m\left(q(t+\tau-kT)-q(t-kT)\right)\right).$$

Furthermore, the autocorrelation function $R(\tau)$ of $s(t)$ is given as

$$R(\tau) = \frac{1}{T}\int_0^T R(t+\tau,t)dt.$$

Finally, the power spectrum corresponds to the Fourier transform of the autocorrelation function $R(\tau)$.

Figure 9 shows the one-sided power spectrum of a 4-level CPFSK signal with symbol duration T = 0.75 ns, $B_{3dB}T$ = 3, and modulation index h = 0.47, computed numerically according to the above procedure. The theoretical signal bandwidth is of course infinite. The 99%-bandwidth, i.e., the bandwidth including 99% of the signal power, may be used to quantity the bandwidth consumption of a signal. In the case of Figure 9, the 99%-bandwidth is approximately 3 GHz.

A symbol duration of T = 0.75 ns as chosen above results in a baud rate of 4/3 GHz, and a raw bit rate of 4 Gbit/s is achievable by employing 8-level modulation. The bandwidth usage depends on the modulation index and the modulation level. A small h keeps the bandwidth low, at the cost of error rate performance as has been seen in the previous section. Figure 10 shows the 99%-bandwidth versus the modulation index for employing a Gaussian low-pass filter with $B_{3dB}T$ = 0.5. Obviously, a 4-ary CPFSK signal occupies about twice the bandwidth of a binary modulated CPFSK signal, and the bandwidth approximately doubles again in the case of 8-level modulation. However, the 99%-bandwidth is a non-linear function of h. Figure 11, Figure 12, and Figure 13 show the corresponding results for $B_{3dB}T$ equal 1.0, 2.0, and 3.0, respectively. An increase in bandwidth consumption by about 10% is found from Figure 10 to Figure 11, whereas for $B_{3dB}T$ above 2.0 the bandwidth does not essentially increase. For the extreme case with $B_{3dB}T$ = 100, the bandwidth is shown in Figure 14.

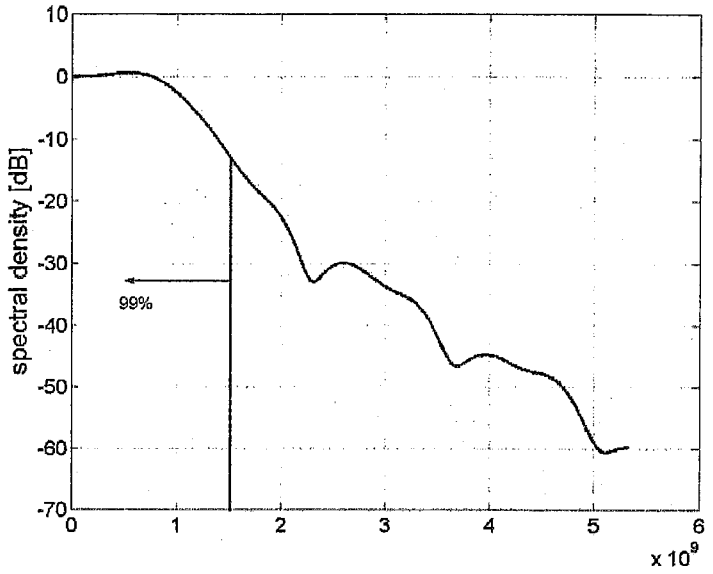

Figure 9: One-sided spectral density for $T^{-1} = 1.333$ GHz, $B_{3\text{dB}}T = 3$, $h = 0.47$, $M = 4$.

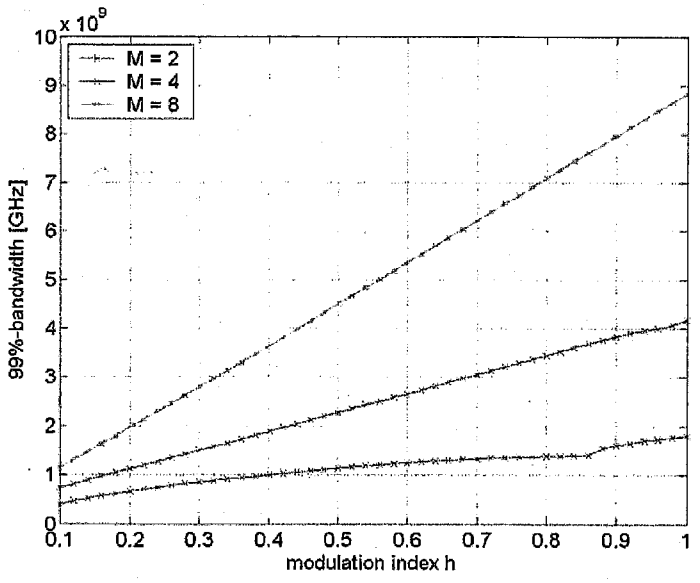

Figure 10: 99%-bandwidths for $T^{-1} = 1.333$ GHz, $B_{3\text{dB}}T = 0.5$.

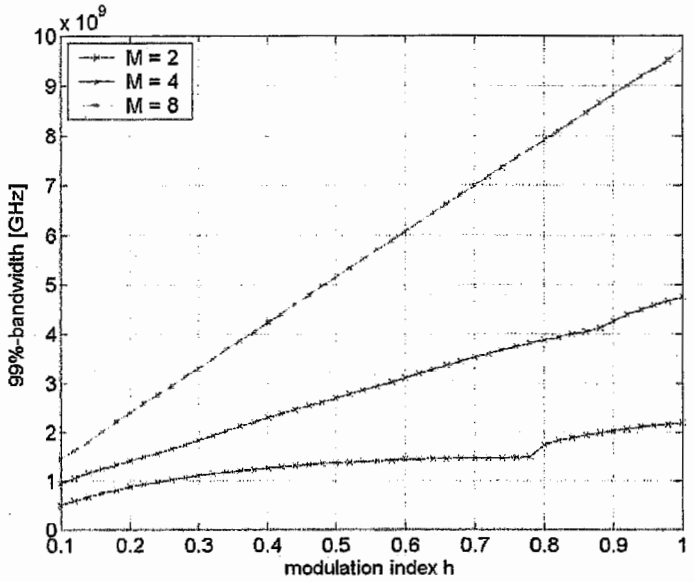

Figure 11: 99%-bandwidths for T^{-1} = 1.333 GHz, $B_{3dB}T$ = 1.0.

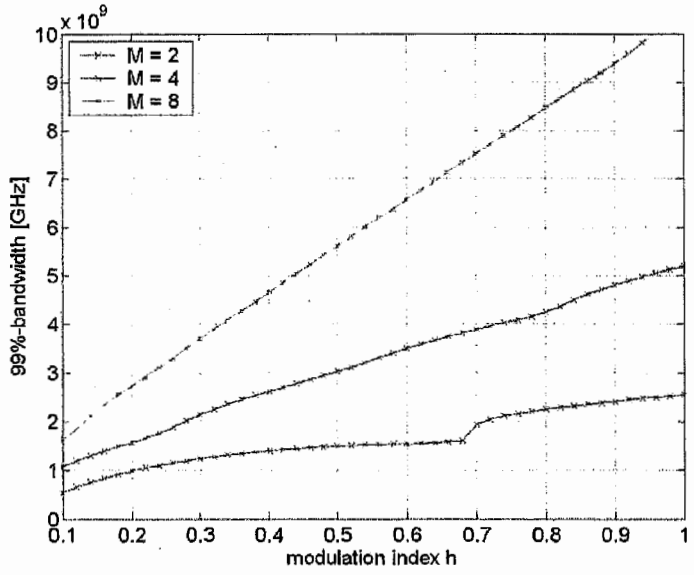

Figure 12: 99%-bandwidths for T^{-1} = 1.333 GHz, $B_{3dB}T$ = 2.0.

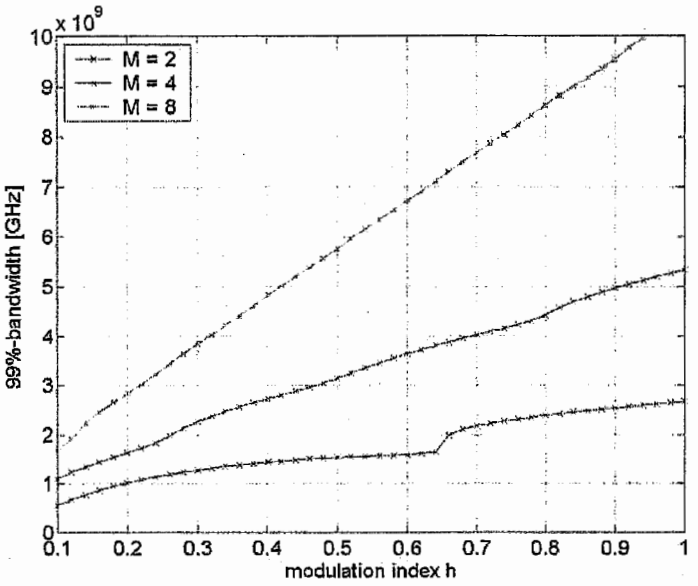

Figure 13: 99%-bandwidths for T^{-1} = 1.333 GHz, $B_{3dB}T$ = 3.0.

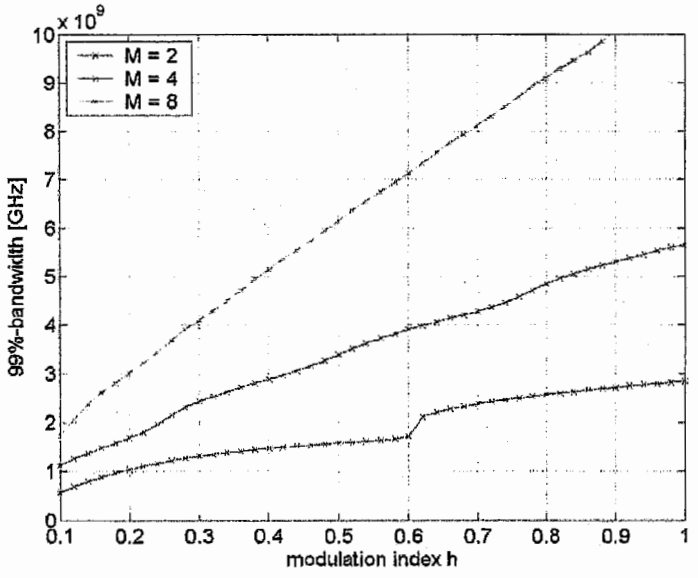

Figure 14: 99%-bandwidths for T^{-1} = 1.333 GHz, $B_{3dB}T$ = 100.

6. System Parameters for a 4-Gigabit WLAN

Based on the results in the previous sections, the adequate parameters for an envisaged CPFSK-based system can be found. As above, a fixed symbol rate of 1.333 GHz is assumed, achieving 4 Gbit/s raw data rate if using 8-level CPFSK. To cope with varying SNR, 4-level or binary modulation shall be alternatives, resulting in 2.667 Gbit/s and 1.333 Gbit/s, respectively. The 99%-bandwidth shall be restricted to 3 GHz in this case study. And the low-pass filter shall also be fixed. As $B_{3dB}T$ products of 0.5 and 1.0 result in poor error rate performance with 8-level modulation, the $B_{3dB}T$ product is assumed either 2.0 or 3.0.

For the case of $B_{3dB}T$ = 2.0, the maximal modulation index fulfilling the bandwidth limitation of 3 GHz equals h = 0.23 for 8-ary CPFSK and h = 0.495 for 4-ary CPFSK, as can be seen in Figure 12. As the error rate performance improves with h, those are the optimal choices. For binary modulation, the bandwidth constraint is fulfilled even for h larger than one. The error rate decreases when the modulation index goes beyond 1, hence, choosing h = 1 is optimal in the case of binary CPFSK. Figure 15 shows the SERs for the three modulation schemes with the optimized modulation indices versus the SNR. Furthermore, Table 1 summarizes the data rate, bandwidth, optimal modulation index, and the required SNR for attaining a BER below 10^{-3} for $B_{3dB}T$ = 2.0. The corresponding SER results and transmission schemes for the case of $B_{3dB}T$ = 3.0 are shown in Figure 16 and Table 2.

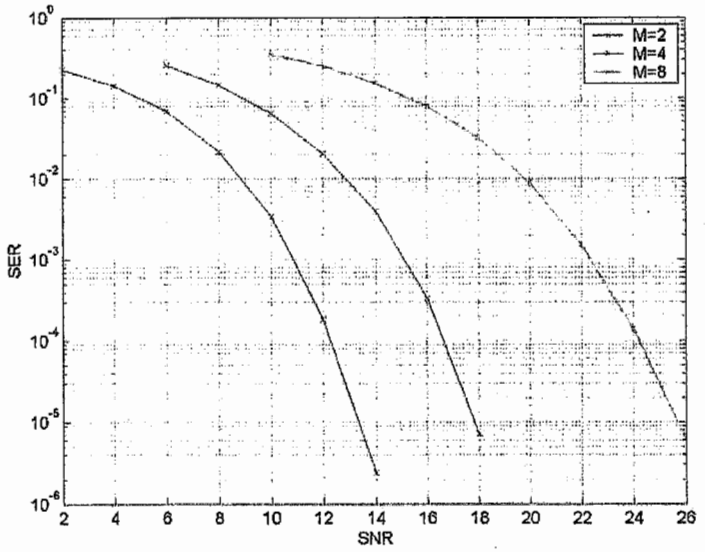

Figure 15: Symbol error rates for $B_{3dB}T$ = 2, h = 1 / 0.495 / 0.23.

modulation level M	data rate	bandwidth	modulation index h	ε_S/N_0 for SER $< 10^{-3}$
2	1.333 Gbit/s	3 GHz	1.0	11 dB
4	2.667 Gbit/s	3 GHz	0.495	15 dB
8	4 Gbit/s	3 GHz	0.23	22.5 dB

Table 1: Optimized transmission schemes for $B_{3dB}T = 2$.

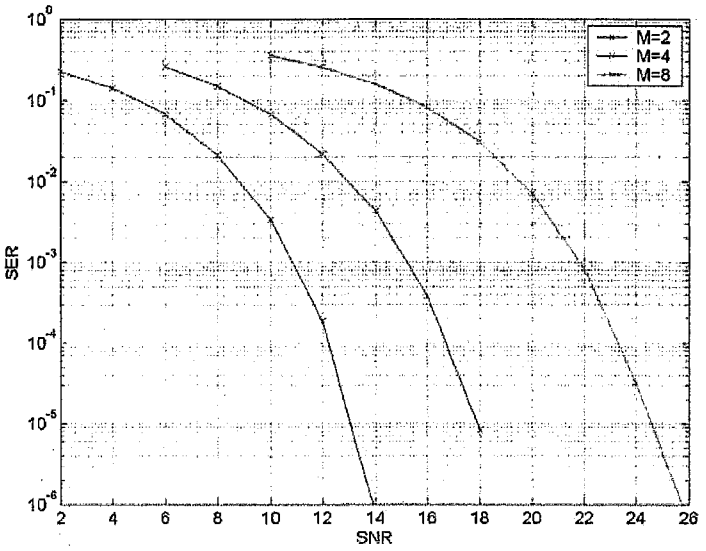

Figure 16: Symbol error rates for $B_{3dB}T = 3$, $h = 1 / 0.47 / 0.217$.

modulation level M	data rate	bandwidth	modulation index h	ε_S/N_0 for SER $< 10^{-3}$
2	1.333 Gbit/s	3 GHz	1.0	11 dB
4	2.667 Gbit/s	3 GHz	0.47	15 dB
8	4 Gbit/s	3 GHz	0.217	22 dB

Table 2: Optimized transmission schemes for $B_{3dB}T = 3$.

7. Summary & Conclusions

As an auspicious modulation method for WLANs in millimeter-wave bands providing data rates in the Gbit/s range, CPFSK has been investigated in this report. The error rate performance of CPFSK signals in combination with noncoherent receivers, and their bandwidth consumption has been calculated. Based on the obtained results, adequate transmission schemes have been identified for achieving data rates up to 4 Gbit/s at bandwidths of at most 3 GHz and SERs below 10^{-3} without forward error control coding. With the assumed theoretical noncoherent receiver and 8-level CPFSK, an SNR of 22 dB has turned out necessary in ideal channels. An equivalent transmission with binary or 4-ary CPFSK, attaining bit rates of 1.333 Gbit/s or 2.667 Gbit/s, requires 11 dB or 15 dB, respectively, to achieve SERs below 10^{-3}.

References

[1] T. Ohira, "Prospective System Design for Gigabit Rate Wireless Local Area Networks", to be presented at the *Int. Joint Conf. of the MINT Millimeter-Wave Int. Symposium (MINT-MIS2005) and the Topical Symposium on Millimeter Waves (TSMMW2005)*, Seoul, Korea, Feb. 2005.

[2] J. G. Proakis, "Digital Communications", 3rd ed., McGraw-Hill.

[3] M. K. Simon and C. C. Wang, "Differential Versus Limiter-Discriminator Detection of Narrow-Band FM", *IEEE Trans. Commun.*, vol. 31, no. 11, Nov. 1983.